S. BESNER
A.V. KABASHIN✉
M. MEUNIER✉

Two-step femtosecond laser ablation-based method for the synthesis of stable and ultra-pure gold nanoparticles in water

Laser Processing Laboratory, Department of Engineering Physics, École Polytechnique de Montréal, Case Postale 6079, succ. Centre-ville, Montréal (Québec), Canada, H3C 3A7

ABSTRACT A two-step laser-assisted method for the synthesis of small and low-dispersed colloidal gold nanoparticles in deionized water is reported. As the first step, laser ablation from a gold target is used to fabricate relatively large (few tens of nanometers) and size-dispersed colloids. As the second step, self-modification of the femtosecond laser pulse into a white-light supercontinuum is used to perform the secondary ablation of colloids. We show that the latter treatment leads to a drastic reduction of both the mean nanoparticles size and size dispersion as well as to the enhancement of the solution stability. Being prepared in pure deionized water, the colloidal nanoparticles are stable and free of any impurities, making them unique for surface enhanced Raman scattering (SERS) and bio-imaging in vivo applications.

PACS 81.05.-t; 82.70.Dd

1 Introduction

Supporting localized light-induced plasmon oscillations, metal nanoparticles exhibit a number of unique optical properties such as, e.g., the dependence of optical extinction spectra on the size and shape of nanoparticles [1, 2], as well as strong field enhancement effects [3, 4]. These properties make the nanoparticles exceptional candidates for ultrasensitive chemical characterization, biosensing and imaging. Such applications generally require an ultra-pure metal surface, free of any contaminant. However, the fabrication of such surfaces is problematic by conventional chemical synthesis routes, since they always lead to surface contamination, mainly by residual anions and by the reducing agent [5, 6].

When performed in deionized water in the absence of chemical additives, laser ablation has proved itself as a unique tool to solve surface contamination (for review, see e.g. [7]). However, a fast coalescence and agglomeration of ablated species generally leads to a broadened size distribution of nanoparticles with a mean size between a few ten and a few hundred nanometers [8–13]. In order to control the nanoparticle size distribution produced by the laser ablation, we recently proposed the use of femtosecond laser radiation [14–18], which exhibits a much higher threshold of cavitation phenomena [19] and a higher energy of ablated

✉ Fax: 1-514-3403218, E-mail: michel.meunier@polymtl.ca

species [20]. Ablation by femtosecond radiation near the threshold led to a drastic decrease of nanoparticle size to 4–5 nm and size dispersion to 2 nm FWHM, which is barely possible with nanosecond laser ablation. However, small size and low dispersion was compromised by a very slow production rate because of small laser fluences. In fact, the fabrication of every sample took up to 6–8 h of ablation at a repetition rate of 1 kHz to produce a reasonably high concentration of nanoparticles. Such slow production efficiency hardly appeared consistent with the necessity of mass nanoparticle production for different applications.

In this article, we report a two-step laser-assisted method, which drastically accelerates the synthesis of small and low size-dispersed colloids in pure deionized water.

2 Experimental setup

The synthesis of the colloidal gold nanoparticles was carried out using a pulsed Ti:sapphire laser (Hurricane, Spectra Physics Lasers) operating at 1 kHz with a pulse width of 140 fs and consisted of the ablation from a gold pellet (99.99%) and the post fragmentation of the produced colloids in a solution. The size distribution of the nanoparticles was examined by transmission electron microscopy (TEM). Solutions of nanoparticles were dropped on a carbon-coated, formvar-covered copper grid and air dried. The size and the size distribution were obtained by measuring the diameter of more than 600 particles observed in different areas of the copper grid. UV-visible extinction spectra of the colloidal solutions were recorded using a Hewlett Packard 8452A Diode Array Spectrophotometer.

3 Results

The proposed laser-assisted nanofabrication procedure consisted of two steps. In the first "laser ablation" step, we used a methodology described in our previous papers [14, 15, 18]. Briefly, the gold target was placed at the bottom of a glass vessel filled with 20 mL of highly deionized water (18.2 MΩ cm) and was irradiated for 10 min with a pulse energy of 500 μJ which was focused onto a spot size of 200 μm on the target using a lens with a focal length of 750 mm. The target was also moved at a scanning speed of 0.35 mm/s in the focusing plane to obtain identical surface conditions during the laser ablation. As we previously showed [15, 18], such ablation generally leads to rapid production of gold colloids with a broad size distribution.

The ablation process was accompanied by the presence of an intense plasma plume and by an audible whistling. In this regime, the solution turned purple a few minutes after the beginning of ablation. As shown in Fig. 1, TEM images of nanoparticles synthesized by laser ablation showed the presence of large and strongly dispersed nanoparticles. These large colloids were interlinked by a large amount of smaller particles to form big aggregates in the solution. As follows from statistical size analysis, the mean size and size dispersion were 55 nm and 34 nm, respectively. As shown in Fig. 2 ($t = 0$), the extinction spectrum of this initial solution was characterized by the presence of a broad plasmon-related peak centered at 536 nm. By comparing such a broad and red-shifted peak to one of the small 3–30 nm nanoparticles (520 nm), we can conclude the presence of a certain "dephasing" of signals from individual plasmons due to an increase of particle size and size dispersion, as well as the nanoparticles agglomeration [1].

During the second "laser treatment" step, smaller portions of the newly prepared solution were transferred in a smaller quartz cuvette with an optical path length of 20 mm and were subjected to laser irradiation. Radiation from the femtosecond laser with a pulse energy of 500 µJ was focused in the cuvette containing the nanoparticle solution down to a spot size of 250 µm at the cuvette exit (water/glass interface). To ensure homogenous laser irradiation of the colloids, the solution was stirred by a small bar magnet at a speed of 700 rpm.

Throughout the second irradiation treatment, we could see a strong scattering of the initial pumping radiation in the propagation pathway of the laser beam using a sensitive CCD camera in the near infrared. However, the scattering intensity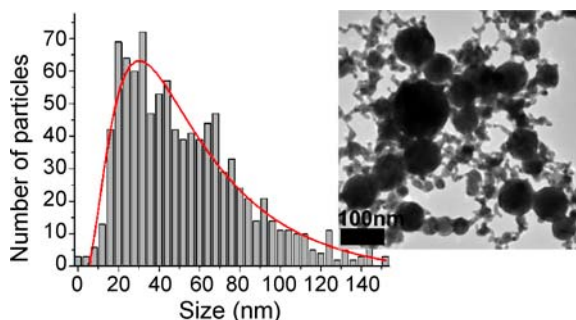 rapidly decreased, indicating a weaker interaction between the fragmented nanoparticles in the solution and the initial 800-nm radiation. A strong white-light composed of multiple filaments could also be seen in the last 7 mm of the beam propagation in the water cuvette. This generation of white-light is generally associated with the self-transformation of the initial radiation due to the strong non-linear interaction with the liquid. The maximum intensity achieved in the water cuvette was $(1.4 \pm 0.3) \times 10^{12}$ W/cm^2, which is lower than the threshold of optical breakdown in water $(1.11 \times 10^{13}$ W/cm$^2)$ [21] but higher than the power threshold (4.4 MW) [22] of the phenomena of laser filamentation, self-focusing and supercontinuum generation. No bubble formation or strong local scattering of this white-light were found, confirming the absence of any optical breakdown in the liquid.

During the first minutes of the laser irradiation treatment, the solution color rapidly changed from purple to pink-purple with some yellow tint. This color change was accompanied by a sharp increase of the plasmon peak in the extinction spectra (Fig. 2; $t = 15$ min). As shown in Fig. 3a, TEM micrograph revealed a significant decrease of particle agglomeration compared to the initial solution after 15 min of laser irradiation. The large portion of 5–20 nm gold nanoparticles released into the solution was attributed to the fragmentation of the small nanoparticle network shown in Fig. 1. Further irradiation up to 120 min led to a slower but gradual change of the solution color from pink-purple to clear red. This later color change
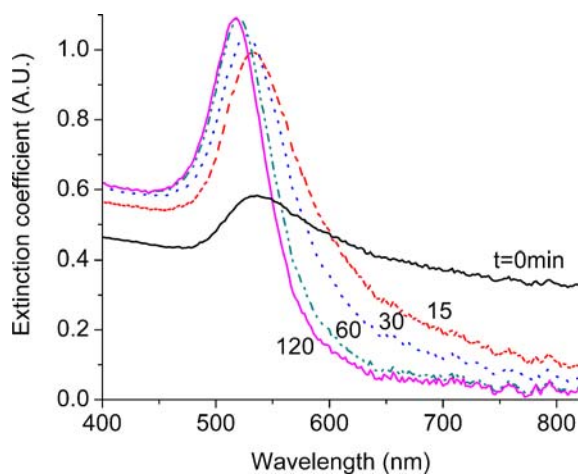

FIGURE 1 TEM micrograph image and corresponding size distribution of nanoparticles produced by laser ablation in deionized water (1st step)

FIGURE 2 Evolution of the extinction spectra as a function of the laser irradiating time during the second "laser treatment" step ($t = 0$, 15 min, 30 min, 60 min, 120 min)
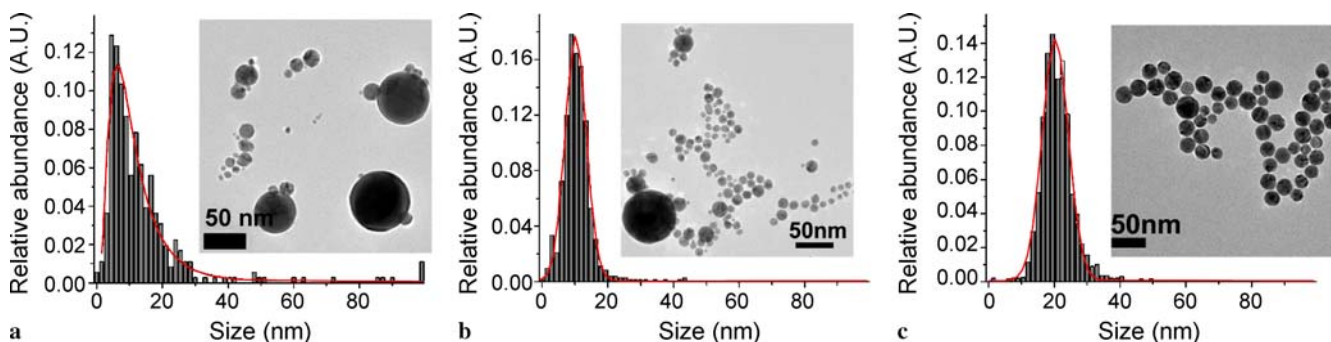

FIGURE 3 TEM micrograph images and corresponding size distributions after 15 min (a), 30 min (b) and 2 h (c) of laser irradiation of the laser synthesized nanoparticles

was accompanied by a monotonous blue shift and amplification of the plasmon-related peak in the extinction spectra, as well as a decrease of the extinction intensity in the range of 600–800 nm (Fig. 2). Such a change in the spectrum suggested a transformation of the large particles into smaller ones ($D < 30$ nm) and a decrease of the size dispersion and agglomeration. This supposition was confirmed by a detailed TEM analysis of nanoparticle size (Fig. 3 b,c). After 30 min, most of the larger colloids were depleted and the mean size was (11 ± 5) nm. The small colloids then started to grow, forming almost perfectly spherical nanoparticles with a mean size of (21 ± 6) nm. The complete time dependence of the size modification is given in Fig. 4. As shown in this figure, after a rapid size reduction during the first 30 min, subsequent laser treatment resulted in a certain increase of the mean size of nanoparticles, finally stabilizing around 20–30 nm.

Our experiments also showed that the treatment radically improved the stability of colloidal nanoparticle solutions. While the initial as-prepared samples precipitated within a few hours, samples treated by 1-h supercontinuum processing showed no sign of precipitation several months after the preparation. This degree of gold nanoparticle stability in the absence of a protective agent is not found in the literature.

4   Discussion

In previous studies [14, 15, 18], we have shown that the size of the gold nanoparticles produced by femtosecond laser ablation ("laser ablation" step) strongly depends on the laser energy, focus conditions and the presence of chemical additives. In this particular case, the initial broad size distribution can be attributed to the plasma related removal of material and to the post-ablation coalescence of the ablated hot nanoclusters during their cooling in the aqueous environment [15, 18]. Due to the high hydrostatic pressure, a large concentration of hot ablated nanoclusters was confined in a small volume at the solid-water interface, which increased the probability of coalescence and particle growth.

In the absence of the phenomenon of optical breakdown in the liquid, the fragmentation process during the "laser treatment" step must be related to the interaction between radiation and nanoparticles. In general, three different contributions can be responsible for the absorption of energy by the nanoparticles:

1. direct absorption of the laser radiation,
2. absorption of energy of the white continuum and
3. interband resonant multiphoton absorption.

As we showed in [23], the third mechanism may be disregarded since the efficiency of multiphoton absorption is negligible for laser intensities used in this study. The first mechanism is related to the absorption of the 800 nm pumping radiation. For spherical gold nanoparticles smaller than 100–200 nm, this absorption is known to be very weak [1, 2]. However, the presence of agglomerates could make this effect significant [24]. Indeed, the elongated nanoparticles forming the network structure are similar to nanorods, which are known to strongly absorb at 800 nm [25]. The second mechanism is related to a nonlinear optical interaction between the radiation and the medium, which strongly modifies the spectral features of the initial laser pulse. Spectroscopic data on

white-light produced at the end of the water cuvette revealed a large broadening of the pulse from ~ 400 nm to ~ 1200 nm with a maximum intensity around 800 nm. The large blue wing was produced mainly by the free-electron generation while the red wing was a combined effect of the instantaneous and delayed responses of the Kerr nonlinearity [26]. The starting point of the supercontinuum generation and its spectral features depend on both the laser energy and the focusing condition. Liu et al. [26] have shown that the spectral broadening increases under the increase of the pulse energy and tight focusing. In this case, a sharp increase of the white-light energy occurs at a very short distance. Our estimations show that about 10% of the initial energy centered at 800 nm was transferred under our experimental conditions into the spectral band of 400–600 nm.

We propose that the fragmentation of nanoparticles in our experiments could be caused by the first two mechanisms. Thus, we reason that the first rapid size reduction is mostly related to the absorption of the 800 nm pumping radiation (Fig. 4). This absorption resulted in the fast fragmentation of the nano-network and a large production of spherical nanoparticles in the range of 5–15 nm. Due to this process, the fragmentation rate then decreased significantly, as the absorption cross-section of separated gold nanospheres in the range of 5–100 nm is very small for 800 nm radiation. However, the spectral broadening of the initial pulse enhanced the total energy transfer as the blue wing of the white-light pulse approached the plasmon related absorption peak of nanoparticles. As shown in [23], this contribution is predominant for spherical nanoparticles smaller than 60 nm. Therefore, in the second size-reduction phase, the fragmentation of separated nanoparticles must be related to their interaction with the white-light pulse. Here, we propose that the fragmentation itself was caused by Coulomb explosion [27–29]. This hypothesis is confirmed by the absence of intermediate size nanoparticles even for a short irradiation time which would be attributed to the thermal evaporation pathway of size reduction.

The final size distribution was almost independent of the initial size and shape of the nanoparticles, but dependent on the radiation parameters and on conditions of coalescence of the fragmented species in the solution. After two hours of laser irradiation, the first fragmented species in the range of
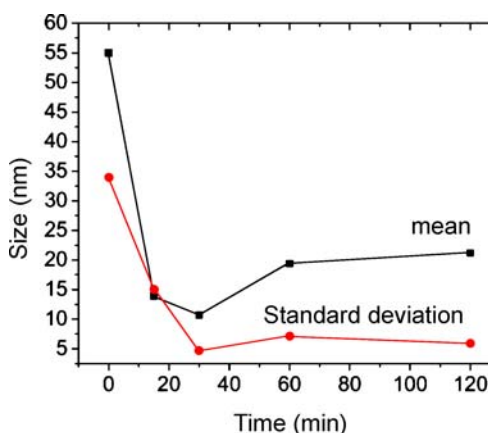

FIGURE 4   Evolution of the mean size and standard deviation as a function of the laser fragmentation duration

1–10 nm were depleted and coalesced into larger nanoparticles with a diameter of approximately 20 nm, while further laser treatment did not significantly change the size distribution. These results indicated that the final size distribution depended on the fragmentation rate of the larger nanoparticles and the coalescence rate of the smaller ones.

Finally, the improvement of solution stability was probably related to the increase in the surface charge and to the surface oxidation of the gold nanoparticles. It is well known that the surface charge increases as the size of the particles decreases, leading to a more pronounced coulombic repulsion. X-ray photoelectron spectroscopy data (not shown) also showed an increase of the particle oxidation with the processing time. Similar analysis has previously shown that hydroxylation of an oxidized group at the gold surface raises the surface charge and enhances the wetting of the surface, limiting the particle agglomeration [16].

5   Conclusion

A laser-assisted method to produce ultra-pure colloids with controllable size and size dispersion in neutral aqueous environment has been developed. The method does not require a specific initial nanoparticle size and does not involve any additional chemical agent. When synthesized in pure deionized water, the nanoparticles have unique surface chemistry, not reproducible with any other chemical nanofabrication routes, making them unique for SERS and bio-imaging in vivo applications.

REFERENCES

1 U. Kreibig, M. Vollmer, *Optical Properties of Metal Clusters* (Springer, Berlin, 1995)
2 M. Kerker, *The Scattering of Light and other Electromagnetic Radiation* (Academic Press, New York, 1969)
3 S. Nie, S.R. Emory, Science **275**, 1102 (1997)
4 S. Schultz, D.R. Smith, J.J. Mock, D.A. Schultz, Proc. Nat. Acad. Sci. USA **97**, 996 (2000)
5 A.M. Derfus, W.C.W. Chan, S.N. Bhatia, Nano Lett. **4**, 11 (2004)
6 A. Fojtik, A. Henglein, Ber. Bunsenges. Phys. Chem. **97**, 252 (1993)
7 A.V. Kabashin, M. Meunier, In: *Recent Advances in Laser Processing of Materials*, ed. by J. Perriere, E. Millon, E. Fogarassy (Elsevier Science Publishing Company, Oxford, 2006)
8 M.S. Yeh, Y.S. Yang, Y.P. Lee, H.F. Lee, Y.H. Yeh, C.S. Yeh, J. Phys. Chem. B **103**, 6851 (1999)
9 F. Mafune, J. Kohno, Y. Takeda, T. Kondow, H. Sawabe, J. Phys. Chem. B **104**, 9111 (2000)
10 F. Mafune, J. Y. Kohno, Y. Takeda, T. Kondow, H. Sawabe, J. Phys. Chem. B **105**, 5114 (2001)
11 A.V. Simakin, V.V. Voronov, G.A. Shafeev, R. Brayner, F. Bozon-Verduraz, Chem. Phys. Lett. **348**, 182 (2001)
12 T. Tsuji, K. Iryo, N. Watanabe, M. Tsuji, Appl. Surf. Sci. **202**, 80 (2002)
13 S.I. Dolgaev, A.V. Simakin, V.V. Voronov, G.A. Shafeev, F. Bozon-Verduraz, Appl. Surf. Sci. **186**, 546 (2002)
14 A.V. Kabashin, M. Meunier, C. Kingston, J.H.T. Luong, J. Phys. Chem. B **107**, 4527 (2003)
15 A.V. Kabashin, M. Meunier, J. Appl. Phys. **94**, 7941 (2003)
16 J.P. Sylvestre, S. Poulin, A.V. Kabashin, E. Sacher, M. Meunier, J.H.T. Luong, J. Phys. Chem. B **108**, 16 864 (2004)
17 J.P. Sylvestre, A.V. Kabashin, E. Sacher, M. Meunier, J.H.T. Luong, J. Am. Chem. Soc. **126**, 7176 (2004)
18 J.P. Sylvestre, A.V. Kabashin, E. Sacher, M. Meunier, Appl. Phys. A **80**, 753 (2005)
19 A. Vogel, J. Noack, K. Nahen, D. Theisen, S. Busch, U. Parlitz, D.X. Hammer, G.D. Noojin, B.A. Rockwell, R. Birngruber, Appl. Phys. B **68**, 271 (1999)
20 J. Perriere, E. Millon, W. Seiler, C. Boulmer-Leborgne, V. Craciun, O. Albert, J.C. Loulergue, J. Etchepare, J. Appl. Phys. **91**, 690 (2002)
21 J. Noack, A. Vogel, IEEE J. Quantum Electron. **35**, 1156 (1999)
22 W. Liu, O. Kosareva, I.S. Golubtsov, A. Iwasaki, A. Becker, V.P. Kandidov, S. Chin, Appl. Phys. B **76**, 215 (2003)
23 S. Besner, A.V. Kabashin, M. Meunier, Appl. Phys. Lett. **89**, 233 122 (2006)
24 W. Rechberger, A. Hohenau, A. Leitner, J.R. Krenn, B. Lamprecht, F.R. Aussenegg, Opt. Commun. **220**, 137 (2003)
25 P.K. Jain, K.S. Lee, I.H. El-Sayed, M.A. El-Sayed, J. Phys. Chem. B **110**, 7238 (2006)
26 V.P. Kandidov, O.G. Kosareva, I.S. Golubtsov, W. Liu, A. Becker, N. Akozbek, C.M. Bowden, S.L. Chin, Appl. Phys. B **77**, 149 (2003)
27 P. Grua, J.P. Morreeuw, H. Bercegol, G. Jonusaskas, F. Vallee, Phys. Rev. B **68**, 12 (2003)
28 P.V. Kamat, M. Flumiani, G.V. Hartland, J. Phys. Chem. B **102**, 3123 (1998)
29 K. Yamada, Y. Tokumoto, T. Nagata, F. Mafune, J. Phys. Chem. B **110**, 11 751 (2006)